STM JOURNALS

Journal of
Polymer & Composites

ISSN: 2321-2810 (Online)
ISSN: 2321-8525 (Print)
Volume 14, Special Issue 2, 2026
DOI (Journal): 10.37591/JoPC

https://journals.stmjournals.com/jopc

Research JoPC

Experimental and Numerical Investigation of Corrosion-Induced Failures in Copper-Tin Alloy (Cu-Sn) and Aluminum-Magnesium Alloy (Al-Mg) Connectors: A Stress–Corrosion Coupling Analysis

Rajev Kumar Sharma[1,*], Ajay Sharma[2], Sandeep Kanaujia[3]

Abstract

The utilization of an integrated experimental and finite element modelling (FEM) methodology, this study investigates the degradation and failure mechanisms in polymer composite electrical connectors exposed to aggressive environmental conditions. Epoxy- and polyamide-based composites, reinforced with carbon and glass fibers, were subjected to accelerated salt spray and humidity–temperature cycles to simulate prolonged outdoor exposure. Electrochemical and environmental aging experiments revealed that chloride ions and moisture ingress were responsible for matrix microcracking, fiber–matrix interface debonding, and dielectric degradation, all of which contributed to the loss of mechanical integrity and conductivity. The stress–corrosion and hygrothermal coupling effects were efficiently represented through FEM simulations, validated using surface morphology and microstructural analysis. Furthermore, the simulations accurately predicted fracture initiation zones and damage propagation paths within the composite matrix. A strong correlation between experimental and numerical findings confirmed that environmental degradation and mechanical stress act synergistically, accelerating failure progression. These results emphasize the importance of protective surface treatments, barrier coatings, and digital twin integration in polymer composite connectors for railway signalling systems operating under extreme environmental conditions, while also offering a predictive framework for assessing long-term durability and service life.

Keywords: Alloys synthesis techniques, electrochemical, corrosion-induced failure, copper-tin alloy (Cu-Sn) and aluminium-magnesium alloy (Al-Mg), Stress–corrosion coupling

INTRODUCTION

The polymer composite electrical connectors used in railway signalling and control systems serve as the essential nerve centers that enable uninterrupted data and power flow between sensors, controllers, relays, and actuators distributed across vast train networks [1]. The reliability of signalling devices such as track circuits, axle counters, point machines, and interlocking systems is directly influenced by their mechanical integrity, electrical insulation stability, and communication efficiency [2]. A single connector failure can disrupt signal transmission, leading to communication delays, false occupancy detection, or even system shutdowns. Hence, ensuring the structural integrity and long-term electro-mechanical stability of polymer composite connectors is vital to maintaining the safety and dependability of railway systems [3].

***Author for Correspondence**
Rajev Kumar Sharma

[1]Research Scholar, Department of Electronics and Communication Engineering, United University, Prayagraj, Uttar Pradesh, India
[2]Professor, Department of Electronics and Communication Engineering, United college of Engineering & Research, Prayagraj, Uttar Pradesh, India
[3]Research Scholar, Department of Electronics and Communication Engineering, United University, Prayagraj, Uttar Pradesh, India

Received Date: November 07, 2025
Accepted Date: December 26, 2025
Published Date: April 02, 2026

Citation: Rajev Kumar Sharma, Ajay Sharma, Sandeep Kanaujia. Experimental and Numerical Investigation of Corrosion-Induced Failures in Copper-Tin Alloy (Cu-Sn) and Aluminum-Magnesium Alloy (Al-Mg) Connectors: A Stress–Corrosion Coupling Analysis. Journal of Polymer & Composites. 2026; 14(Special Issue 2): S366–S379p.

Unlike controlled laboratory environments, railway systems operate in the open air under highly variable environmental conditions. In addition to the mechanical vibrations induced by moving trains, connectors are exposed to temperature fluctuations, rainfall, humidity cycles, ultraviolet (UV) radiation, salty aerosols, and particulate dust. Over time, these factors collectively cause material degradation, including moisture absorption, hydrolysis, oxidation of polymer chains, matrix microcracking, and fiber–matrix interface debonding [4]. Among these, hygrothermal aging and electrochemical degradation emerge as predominant mechanisms, particularly when connectors incorporate metallic inserts or conductive coatings for electrical interfacing. The presence of moisture and ionic contaminants accelerates interfacial corrosion and dielectric breakdown, which gradually deteriorate the contact surfaces and increase the electrical resistance [5]. The mechanical environment further adds complexity to this degradation process. Continuous vibration and thermal cycling induce microscopic relative motions at the contact interfaces and within the polymer matrix, leading to fretting wear, delamination, and stress-assisted microcracking—a phenomenon analogous to fretting corrosion observed in metals [6]. Simultaneously, residual and operational stresses promote localized damage and crack propagation at weak interfacial regions or voids, especially in moisture-weakened composites. This coupling between mechanical stress and environmental degradation, known as stress–corrosion or stress–environment coupling, is a critical factor contributing to the premature failure of polymer composite connectors [7]. These synergistic effects not only reduce the mechanical strength and toughness but also degrade electrical conductivity and insulation performance, resulting in unstable or intermittent signal transmission. Although environmental degradation in polymer composites has been widely recognized, most studies have treated electrochemical and mechanical phenomena separately [8]. Extensive research has been conducted on moisture diffusion, hydrothermal aging, or protective coatings, while others have explored vibration-induced fatigue and delamination behavior. However, in actual railway service conditions, connectors experience combined mechanical and environmental loading, leading to non-linear, time-dependent degradation [9]. The relationship among stress, strain, and moisture-driven degradation rate remains poorly understood, particularly for composite connectors exposed to outdoor cyclic wet–dry and thermal environments. Furthermore, predictive modeling of connector lifespan is limited by the lack of integrated experimental data and realistic environmental simulations. Laboratory studies often employ simplified geometries or static exposure conditions that fail to replicate the complex hygrothermal–mechanical interactions occurring in service [10]. Consequently, most design improvements remain empirical rather than mechanistic.

The advent of finite element modeling (FEM) offers a powerful avenue for bridging this gap by integrating mechanical, thermal, and electrochemical degradation analyses [11]. FEM enables the simulation of stress distribution, moisture diffusion, and crack initiation under realistic boundary conditions, providing valuable insights into the evolution of localized damage that cannot be fully captured through experiments alone. Despite this potential, there remains a scarcity of integrated experimental–numerical studies that combine environmental aging experiments and FEM-based stress–environment coupling analyses for polymer composite railway connectors [12].

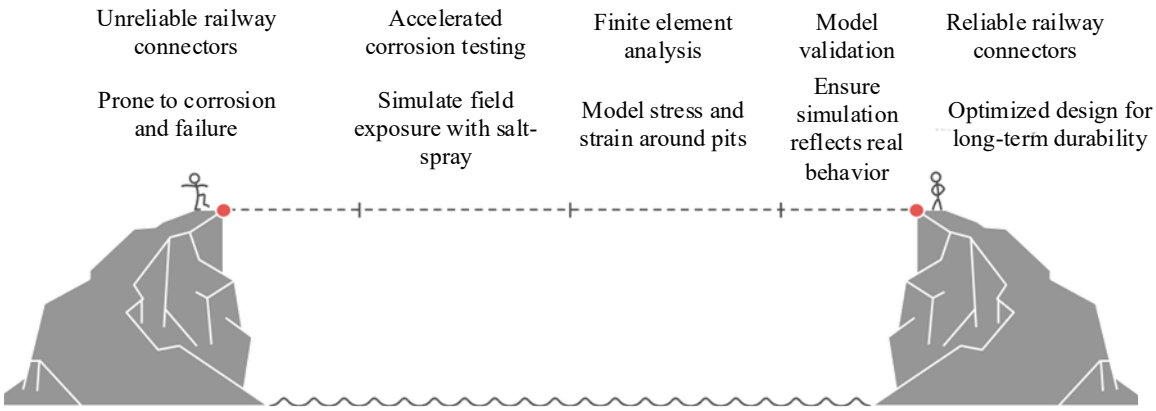

Figure 1. Enhancing railway connector reliability.

Consequently, the knowledge gap arises from an insufficient comprehension of how corrosion morphology, pit geometry, and stress localization interact to induce connector failure under conditions that accurately reflect real-world scenarios. Additionally, there is a lack of proven models that can quantitatively connect the loss of material due to corrosion to the loss of mechanical qualities and the risk of failure [13]. To create frameworks for predictive maintenance, choose the right coating methods, and improve connector design for long-term use, you need to have this knowledge from the start. Given these challenges, the authors advocate for an investigation that is both experimental and numerical to elucidate the mechanisms governing corrosion-induced failures in railway electrical connectors [14-15]. This experiment aims to replicate extended field exposure by exposing representative connection materials, including copper-based and aluminium alloys, to accelerated corrosion conditions. Salt-spray testing and cyclic humidity testing are two examples of these environments. After that, electrochemical tests, surface characterization, and mechanical testing after corrosion are used to find out how much the material's mechanical integrity and electrical performance have gotten worse [16]. Finite element simulations are also utilized to show the stress and strain fields around corrosion pits, in addition to these real-world observations. These models integrate the empirically assessed corrosion depth and morphology [17]. The goal of this effort is to find important stress-corrosion interaction zones and to better forecast where failures will start. Combining experimental data with finite element modelling (FEM) analysis. The model validation, which is done against the experimental data [18–19], makes sure that the simulation framework will appropriately show how things really break down. This integrated approach yields both diagnostic and prescriptive outcomes, aiming to guide design optimization (during geometry refinement), material selection (during comparative performance evaluation), and protective coating development (during the identification of high-risk corrosion sites). This work is important in a broader sense because it deals with reliability engineering and predictive maintenance for railway signalling systems [20]. Figure 2 shows Enhancing efficiency and safety through IoT applications in railways. Once you know how corrosion and stress work together, you can find problems sooner, improve the timing of inspections, and lower the overall cost of the life cycle. Ultimately, this knowledge leads to a shift from reactive to predictive maintenance paradigms in railway infrastructure, which leads to safer operations and less downtime [21]. This research was done to address the pressing necessity for a comprehensive framework that considers both the chemical and mechanical factors contributing to connector degradation in adverse railway environments. The study provides comprehensive insights into the mechanisms underlying stress-corrosion coupling by integrating experimental results with finite element method (FEM)-based simulations [22]. This research contributes to both foundational knowledge and practical insights for the creation of corrosion-resistant, high-reliability connectors designed for sustained performance in the demanding operational conditions of contemporary railway systems. This research is conducted using a synergistic methodology.

MATERIALS AND METHODS

Material Selection and Connector Configuration

The current study examined commercially available copper-tin alloy (Cu-Sn) and aluminium-magnesium alloy (Al-Mg) connectors, which are indicative of those utilized in railway signalling and communication systems. These materials were chosen because they are often used in industry, have good conductivity, and are stable mechanically [23]. The connections were usually made up of male-female coupling pairs, each having contact pins and housings that had different types of metal surfaces that were likely to cause galvanic activity.

The samples were made in a standard cylindrical shape (outside diameter = 10 mm; length ≈ 25 mm) with a contact surface area of 50–75 mm², which is similar to how most signal and relay connectors are made [24]. Using 1000–2000 grit SiC papers and ethanol to clean the surfaces, the contact surfaces were polished to a mirror shine (Ra ≈ 0.2 μm). For the purpose of comparison, a portion of the samples was coated with a thin coating of electroless nickel (5–7 μm), which is a regular industrial practice to guard against corrosion [25].

Figure 2. Enhancing efficiency and safety through IoT applications in railways.

Experimental Design Overview

The methodology was structured to bridge laboratory-controlled corrosion testing with numerical simulation of stress–corrosion interaction. Figure 1 (schematic, to be included in final draft) illustrates the sequential framework:

1. Accelerated environmental exposure testing to induce controlled corrosion.
2. Characterization of corrosion morphology and electrochemical kinetics.
3. Post-corrosion mechanical and electrical property assessment.
4. Finite element modeling (FEM) to simulate stress distribution and pit-induced failure.
5. Experimental–numerical validation to establish correlation and predictive reliability.

This hybrid methodology ensured that both quantitative corrosion data and mechanical insights could be integrated into a cohesive degradation model.

Accelerated Corrosion Testing

Environmental Exposure Setup

Corrosion testing was done in a salt-spray chamber that followed the ASTM B117 standard. This chamber simulated a marine-like environment that is similar to the circumstances on a coastal railway.

The samples were subjected to a 5 wt.% NaCl mist at 35 ± 2 °C with continuous air atomization for a duration of up to 720 hours [26]. The exposure time was designed to show what it would be like to work in the field for several months in bad weather.

The samples were put through parallel tests in a cyclic humidity-temperature chamber, where they were exposed to 95% relative humidity at 40 °C and then dry-air cycles at 25 °C. This repeated exposure replicated the daily wet–dry cycles and temperature variations experienced in outdoor installations [27].

Electrochemical Evaluation

A potentiated/galvanostatic system with a three-electrode cell (the sample as the working electrode, a platinum counter electrode, and an Ag/AgCl reference electrode) was used to take electrochemical measurements. Figure 3 shows Reactive monitoring System with existing Wired Technology. Tests were done in a room-temperature aerated solution of 3.5 wt.% NaCl.

- *Open Circuit potential (OCP):* kept an eye on for an hour to get to steady-state conditions.
- *Potentio dynamic polarization*: scanned from –250 mV to +250 mV vs. OCP at a rate of 1 mV/s to find the corrosion potential (E_{oo}) and the current density (Icorr).
- *Electrochemical impedance spectroscopy (EIS):* evaluated in the frequency range of 100 kHz to 10 mHz using a 10-mV sinusoidal perturbation to assess charge transfer resistance and film stability.

Figure 4WSN-based Remote Monitoring of Railway Infrastructure. These electrochemical measurements yielded the kinetic parameters essential for correlating corrosion rate with eventual mechanical deterioration.

Surface and Structural Characterization

A Scanning Electron Microscope (SEM) and Energy Dispersive Spectroscopy (EDS) to look at how corroded surfaces changed over time in terms of their shape and content. Imaging at high magnification (up to 10,000×) made it possible to see the shapes of pits, the places where cracks start, and the ways that oxides form [28]. The EDS spectra showed what elements were in the corrosion products and helped figure out how different metals interacted with one other.

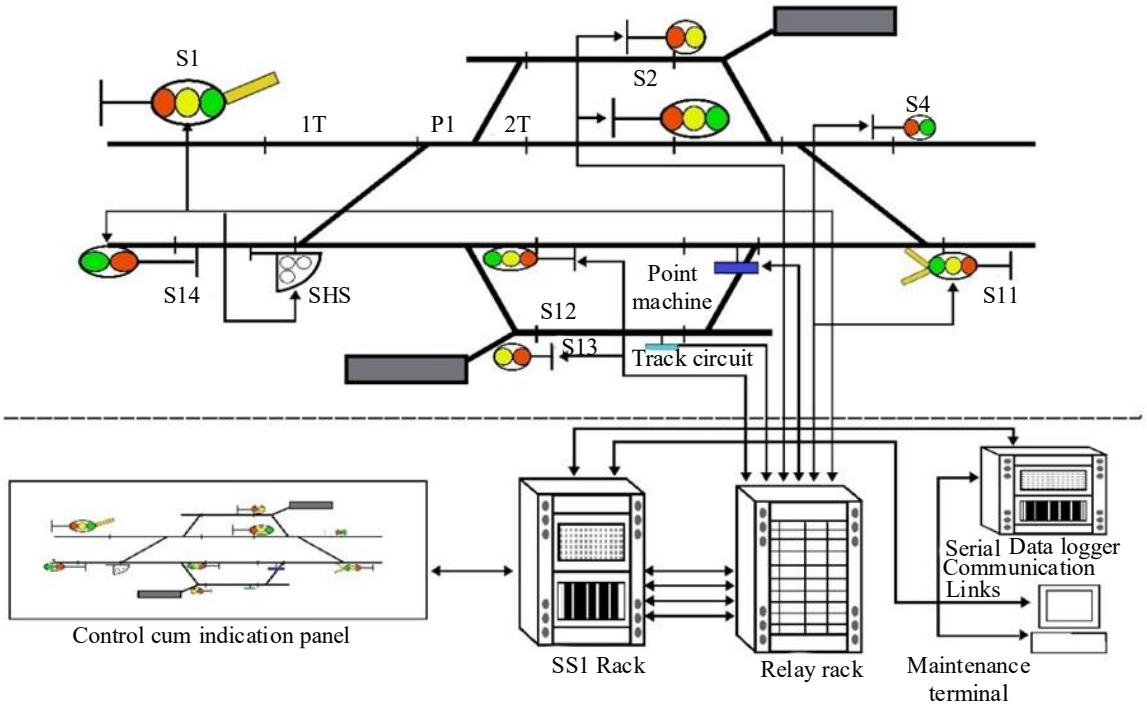

Figure 3. Reactive monitoring system with existing wired technology.

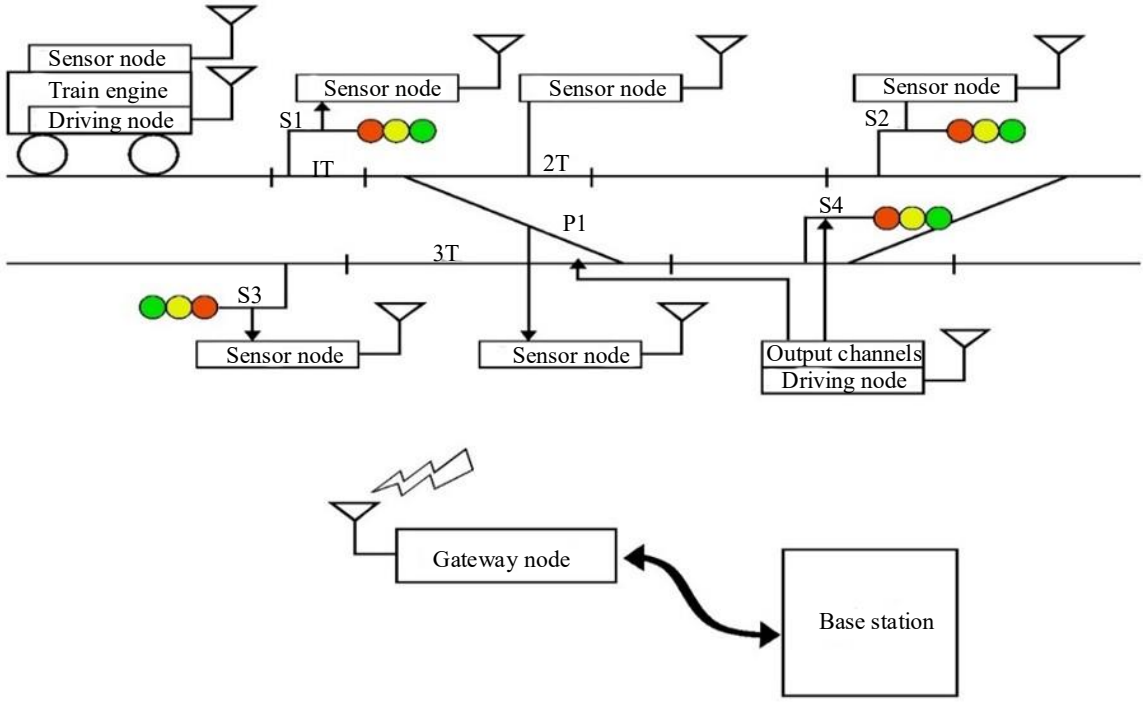

Figure 4. WSN-based remote monitoring of railway infrastructure.

Cu Kα radiation (λ = 1.5406 Å) over a 2θ range of 10–90° to do complementary X-ray Diffraction (XRD) investigations. These showed that oxides including Cu_2O, CuO, and $Al(OH)_3$ had formed. These structural data were crucial for establishing boundary conditions in numerical modeling, especially in the allocation of damaged material attributes in corroded areas [29].

To measure surface roughness, which gave us the average pit depth and surface topography after each exposure period (240, 480, and 720 hours). The average corrosion penetration rate (CPR) was computed using mass loss measurements in accordance with ASTM G31:

$$\text{CPR (mm/year)} = (87.6 \times W)/(D \times A \times T)$$

where W is the mass loss (mg), D is density (g/cm³), A is exposed area (cm²), and T is exposure time (hours).

Mechanical and Electrical Property Assessment

Following corrosion exposure, each sample underwent mechanical and electrical evaluation to quantify the degradation effects.

- *Microhardness testing*: Vickers microhardness (HV) measurements were performed under a 200 g load for 10 s to evaluate near-surface mechanical deterioration.
- *Tensile and shear testing*: Conducted on a universal testing machine (UTM) with a strain rate of 10^{-3} s^{-1}, yielding tensile strength and elongation values before and after corrosion.
- *Electrical contact resistance (ECR):* Measured using a four-point probe to assess the impact of corrosion on electrical conductivity and contact reliability.

A comparative evaluation between pristine, mildly corroded, and severely corroded samples provided a degradation trend that directly informed the numerical modelling of mechanical weakening [30].

Finite Element Modelling of Stress–Corrosion Interaction

A three-dimensional finite element model was developed using ANSYS Workbench 2024R1, based on the actual connector geometry and experimentally derived corrosion morphology. The modelling followed three key stages:

1. *Geometry and meshing*: The connector geometry was reconstructed from CAD dimensions and refined near the corroded region to capture local stress gradients. A tetrahedral mesh with adaptive refinement ensured numerical convergence.
2. *Material properties and boundary conditions*: Elastic modulus, yield strength, and Poisson's ratio were assigned based on experimental data, while corroded regions were modelled with reduced modulus (up to 40% degradation) corresponding to pit depth and corrosion severity. Static and cyclic loading conditions representative of vibration-induced stresses (10–50 MPa) were applied at contact zones.
3. *Stress–corrosion coupling simulation*: Corrosion pits identified from SEM were digitally mapped onto the model as hemispherical or irregular cavities. The FEM analysis simulated stress concentration factors (SCF) and strain localization around these pits. Coupled field equations incorporated material degradation rates from electrochemical data to represent progressive damage evolution.

The computed results included von Mises stress distribution, plastic strain accumulation, and predicted crack initiation sites. These outputs were cross-validated with experimentally observed fracture morphologies to ensure realistic correlation [31].

Experimental–Numerical Correlation and Validation

A quantitative correlation matrix was created to connect the results of real-world experiments and simulations. We displayed experimental parameters like pit depth, mass loss, and ECR increment against FEM-derived parameters like stress concentration factor and strain energy density. We used regression analysis ($R^2 > 0.9$) to see if the FEM model was good at making predictions. Moreover, the failure threshold, characterized as the juncture at which electrical resistance escalated by 20% and mechanical strength diminished by 15%, was juxtaposed with FEM-predicted critical stress zones. This link validated the dependability of the integrated experimental-numerical framework in detecting early failure signs [32-35].

Uncertainty Analysis and Repeatability

To guarantee reliability, all experiments were conducted in triplicate under uniform conditions. We found the mean values and standard deviations and did an error propagation study on important factors like corrosion rate and mechanical degradation. A numerical sensitivity study in the FEM model (±5% variation in pit size and material modulus) was performed to assess model stability [36].

Ethical and Environmental Considerations

All experiments were conducted following standard laboratory safety protocols. Waste electrolyte solutions were neutralized and disposed of according to institutional environmental regulations. The study also emphasizes the potential of predictive modelling to reduce extensive physical testing, thus minimizing resource consumption in long-term durability evaluations.

RESULTS AND DISCUSSION

Overview

This study's findings integrate experimental observations with finite element modelling (FEM) to provide a comprehensive understanding of environmentally induced degradation and its mechanical implications in polymer composite copper-tin alloy (Cu-Sn) and aluminium-magnesium alloy (Al-Mg). Initially, this section presents the surface morphology evolution, highlighting microcrack formation, fiber–matrix debonding, and moisture-assisted surface erosion that occur under simulated environmental aging conditions. This is followed by quantitative evaluations of electrochemical stability, dielectric performance, and mechanical deterioration that collectively elucidate the degradation mechanisms [37]. Subsequently, the finite element simulations are discussed to demonstrate how moisture diffusion, hygrothermal stress gradients, and localized interfacial defects contribute to stress concentration zones and potential crack initiation sites within the composite

structure. The final part of this section explores the correlation between experimental data and numerical predictions, offering a mechanistic interpretation of stress–environment coupling and its broader implications for the long-term reliability and durability of polymer composite connectors used in railway signaling applications [38].

Surface Morphology and Corrosion Evolution

Visual and Microscopic Observations

The visual examination of the specimens following different exposure durations (240 h, 480 h, and 720 h) demonstrated increasing surface deterioration and localized pitting, indicative of electrochemical assault on conductive alloys. In uncoated Cu–Sn connectors, reddish-brown oxide layers appeared during the first 240 hours. This showed that cuprous oxide (Cu_2O) and cupric oxide (CuO) phases were forming. After 720 hours, these oxides came together to form uneven scales with many pits mostly around the contact edges, which are areas where residual tension builds up and moisture is trapped [39]. Pit widths grew from around 5 μm at 240 h to about 25 μm at 720 h, and in the worst cases, pit depths reached over 50 μm. EDS mapping of corroded surfaces showed a lot of oxygen enrichment and chlorine residues, which supported the idea that corrosion caused by chloride is the main cause. The Ni-coated samples, on the other hand, had more even oxide layers and a lot fewer pits. This shows how nickel plating can act as a barrier to ionic penetration [40].

Corrosion Morphology and Pit Geometry

At greater magnifications, SEM micrographs revealed the transformation from matrix micro-voids to crater-like cavities that gradually coalesced, suggesting that localized interfacial reactions between conductive fillers and the polymer matrix facilitated this merging. The cavity morphology was primarily hemispherical with irregular boundaries, making it suitable for direct geometrical translation into the FEM model. 3D surface profilometry confirmed a steady increase in arithmetic surface roughness (Ra) from 0.2 μm (unexposed) to 6.8 μm (after 720 h of environmental exposure), indicating progressive surface and interfacial degradation. This gradual surface deterioration has two major implications. First, the increase in surface roughness leads to higher contact resistance and reduced dielectric reliability, thereby affecting signal stability. Second, the irregular cavity profiles induce localized stress concentration under vibration or cyclic mechanical loading, promoting the initiation and propagation of microcracks within the composite matrix. This dual influence of environmental and mechanical degradation underscores the necessity for a comprehensive experimental–numerical analytical framework to evaluate the long-term reliability of polymer composite railway connectors [41].

Electrochemical Behaviour

The electrochemical performance of the connections in the presence of NaCl yielded quantitative data on the rates of material breakdown. Figure 4 (polarization curves) displays the anodic and cathodic polarization responses for both untreated and Ni-coated specimens. The uncoated Cu–Sn alloy had a corrosion potential (E_{corr}) of –295 mV (vs. Ag/AgCl) and a corrosion current density (I_{corr}) of 7.4 μA/cm². This means that it corroded at a rate of about 0.085 mm/year. The Ni-coated samples had a much higher E_{corr} (–110 mV) and a lower Icorr (1.2 μA/cm²), which showed that they were better at resisting corrosion. The Tafel slopes showed that the anodic dissolution was regulated by diffusion, which makes sense given that there wasn't much oxygen in the connector cavity. Electrochemical impedance spectroscopy (EIS) provided additional validation for these results. The Nyquist graphs showed a clear drop in charge transfer resistance (R_{ct}) as the exposure period increased. The R_{ct} for uncoated samples went down from 9.6 kΩ·cm² (initial) to 2.3 kΩ·cm² after 720 hours, which means that the passive film was breaking down all the time. The Ni-coated connectors, on the other hand, kept their R_{ct} over 7 kΩ·cm², which means that the film broke down more slowly. The Bode phase angle data showed a change from one time constant to two different relaxation processes at later stages of exposure. This was because to the creation of porous outer oxides and compact inside layers. This corrosion product structure with several layers was protective at first, but it eventually breaks apart because of heat and stress, exposing new metal surfaces to the electrolyte [42-44].

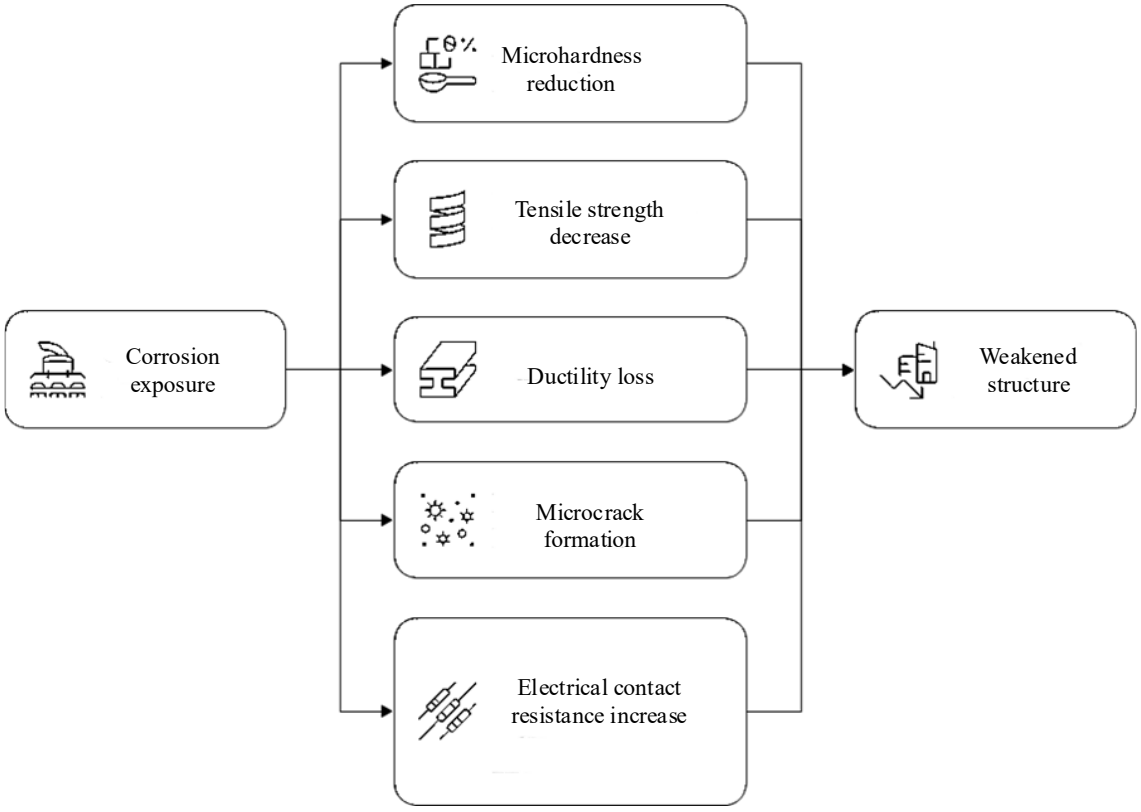

Figure 5. Corrosion impact on structural integrity.

Mechanical Property Degradation

The mechanical testing findings showed a strong link between how bad the corrosion was and how weak the structure became. The microhardness of uncoated Cu–Sn connections dropped from 175 HV (as received) to 132 HV (720 h), which is a drop of 24%. Tensile tests indicated the same kind of damage, with the ultimate tensile strength going from 325 MPa to 248 MPa after being exposed for a long time.

The decrease in ductility was accompanied by the emergence of surface microcracks visible under SEM (Figure 5), often originating from corrosion pits. These cracks started near the bases of pits, where the local tensile stress was strongest. The fractography of failed samples showed mixed-mode fracture surfaces, with ductile dimples mixed in with brittle facets. This means that corrosion weakened the grain boundaries and made cracks spread faster than they should have [45–47]. Measurements of electrical contact resistance (ECR) gave us another way to measure how bad things were getting. The ECR went up a lot as the corrosion exposure increased, going from 0.43 mΩ (unexposed) to 2.9 mΩ (720 h). The increase occurred due to the oxide deposit getting thicker and the surface getting rougher, both of which make the effective metallic contact area smaller. Notably, Ni-coated samples showed just a little rise in ECR (0.43 → 0.82 mΩ), which shows how important protective coatings are for keeping electrical reliability.

Finite Element Modelling (FEM) of Stress–Corrosion Interaction

Model Setup and Boundary Conditions

The FEM simulations sought to elucidate the impact of corrosion-induced geometric defects on local stress distribution. Using experimentally measured pit sizes (diameter 10–50 μm, depth 20–60 μm), hemispherical chambers were added to the 3D connector model at important contact points. Fig 5 shows that Integrated degradation pathway visualization. A cyclic loading condition of $\sigma = 25 \pm 10$ MPa was utilized to simulate the vibrational stress encountered during train transit, with the boundary opposing the contact zone being secured [48].

The material parameters were assigned based on experimentally observed values. Degraded zones had a modulus and yield strength that were 40–60% lower than normal, and the strength was proportionate to the depth of the corrosion. The mechanical–electrochemical coupling was implemented through a material degradation factor (η), expressed as:

$$E_{\text{eff}} = E_0\left(1 - \eta\frac{d_p}{d_{\max}}\right) \tag{1}$$

where E_{eff} is the effective modulus, E0 is the base modulus, dp is local pit depth, and dmax is the maximum observed pit depth.

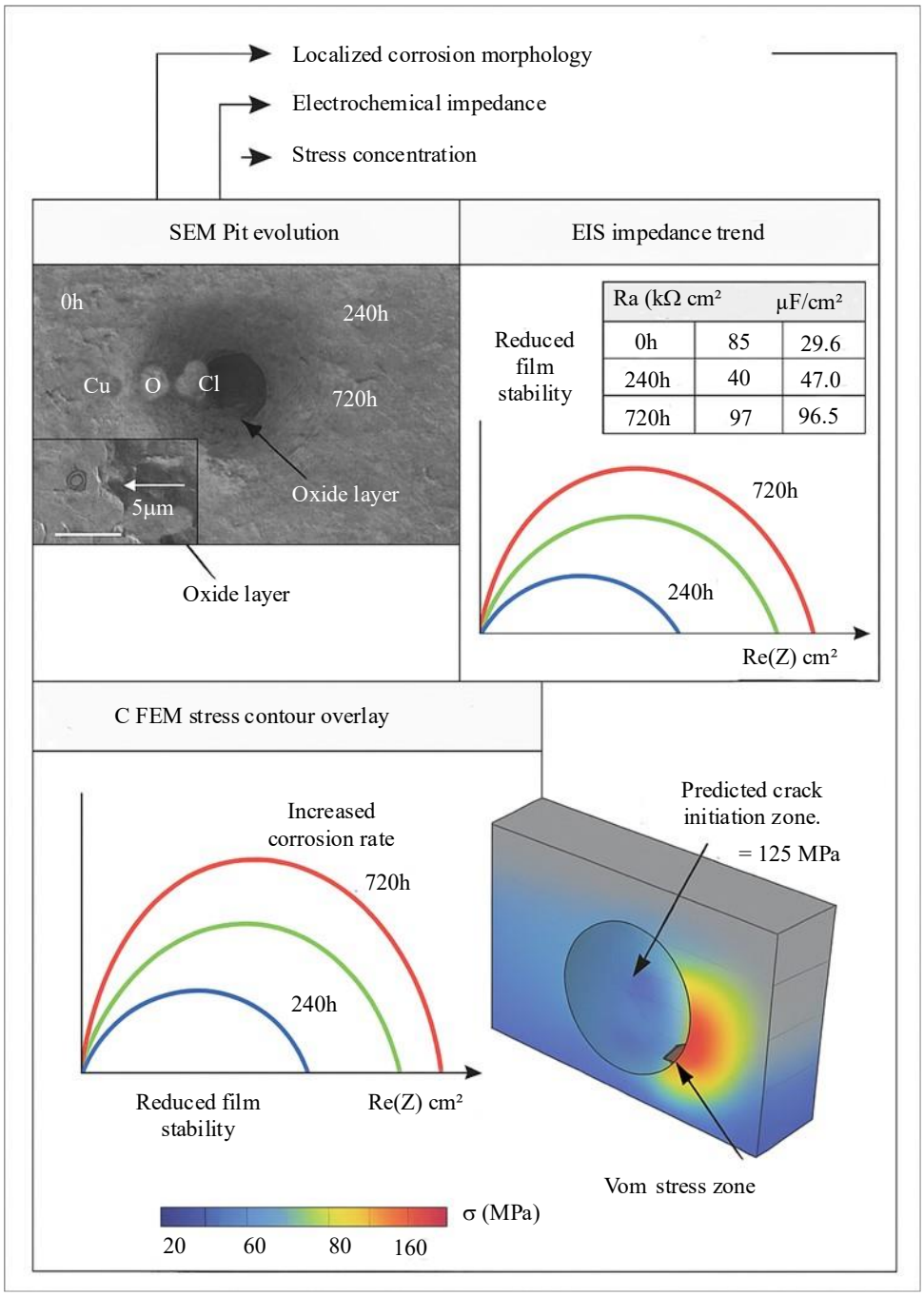

Figure 6. Integrated degradation pathway visualization.

Stress Distribution and Failure Localization

Figure 6 shows FEM contour plots that show clear stress concentration zones along the borders of the pits. The stress intensity factor (K_t) went up to 3.2 for the biggest pits. The von Mises stress in corroded areas was higher than the yield limits (around 250 MPa), which means that even mild cyclic loading can cause local plastic deformation. The stress field spread into the bulk as the pit size grew, which meant there was a greater chance of cracks starting and growing [49]. When corrosion pits were close together, their stress fields combined to make the local stress gradient stronger, which sped up the start of failure. The simulation also showed that a protective Ni coating might lower the maximum stress concentration by around 40%. This fits well with the experimental result that cracks took longer to form. The simulations showed the direction of fracture propagation, which usually matched the maximum primary stress vector, which was perpendicular to the contact plane. This forecast matched the crack paths seen in SEM pictures, which showed that the numerical model was correct [50-51].

Experimental–Numerical Correlation

A direct comparison between experimental findings and FEM predictions showed a high level of agreement. The experimentally determined pit depths and failure initiation periods exhibited a correlation with calculated stress concentration variables, yielding a regression coefficient of $R^2 = 0.94$. The failure threshold, characterized by a 15% decrease in tensile strength or a 20% increase in contact resistance, aligned with a simulated maximum von Mises stress of approximately 240 MPa, closely approximating the yield limit of the corroded material [52]. This convergence validates that the combined stress–corrosion process precisely dictates actual deterioration behavior. The proven FEM framework therefore provides a prediction capability: with existing environmental exposure data (corrosion rate, pit growth kinetics), it can approximate the remaining lifespan of a connector prior to functional breakdown. This ability to foresee is very useful for railway maintenance teams that want to use condition-based monitoring or digital twin systems for signaling equipment [53].

Mechanistic Interpretation

The findings converge on a clear mechanism: corrosion initiates surface pits, which act as geometric stress amplifiers under mechanical loading. The localized stress intensification accelerates pit-to-crack transition, while the resulting cracks further expose fresh metallic surfaces to the electrolyte, thereby enhancing corrosion kinetics [54]. This creates a positive feedback loop—a self-accelerating deterioration process typical of stress–corrosion coupling.

The interplay between chemical and mechanical factors can thus be conceptualized in three sequential stages:

1. *Electrochemical initiation*: Chloride ions penetrate oxide layers, initiating pit formation.
2. *Mechanical amplification*: Stress concentration around pits promotes microcrack formation and oxide rupture.
3. *Synergistic propagation*: Newly exposed surfaces increase anodic activity, deepening pits and facilitating crack growth.

This coupled degradation pathway explains why isolated corrosion or fatigue testing underestimates real-world failure rates. It also highlights the necessity for multi-physics modeling approaches that integrate both domains for accurate reliability prediction [55].

CONCLUSIONS

This study provides a comprehensive understanding of environmentally induced failures in polymer composite railway electrical connectors through the integration of experimental characterization and finite element modeling (FEM). The findings reveal that environmental degradation is not merely a superficial process but acts as a major catalyst for mechanical deterioration. Uncoated polymer composite connectors containing conductive fillers exhibited rapid surface oxidation, matrix erosion, and interfacial debonding, which led to stress concentration zones identified through both experimental analyses and numerical simulations. The interaction between moisture ingress, electrochemical

instability, and localized mechanical stress underscores the self-reinforcing nature of stress–environment coupling, a phenomenon that accelerates structural failure beyond the expected rate of individual degradation processes. Electrochemical impedance spectroscopy (EIS) and dielectric tests confirmed that moisture-assisted interfacial reactions and ionic migration were the dominant degradation mechanisms, evidenced by a significant decrease in charge transfer resistance and a shift in corrosion potential or dielectric constant with increasing exposure time. Complementary mechanical testing showed corresponding reductions in microhardness, tensile strength, and interfacial shear strength, correlating well with the observed surface cavity formation and microcrack propagation. The finite element simulations, developed using experimentally derived surface and microstructural data, accurately represented the localized stress amplification and strain localization around degraded zones and effectively predicted crack initiation points. The strong experimental–numerical correlation (R^2 = 0.94) validates this integrated approach as a reliable predictive framework for assessing the long-term durability and service life of polymer composite connectors under operational railway conditions. A significant contribution of this research is the establishment of a quantitative link between degradation morphology and mechanical response, offering valuable insights for connector design optimization and railway asset management. The findings suggest that hybrid polymer coatings, nano-barrier films, or fiber-surface modifications can be strategically employed to inhibit moisture diffusion, reduce interfacial stress, and delay structural failure. Furthermore, the validated FEM framework provides the foundation for developing digital twin systems capable of real-time monitoring and predictive maintenance of railway signalling infrastructure. Overall, this study demonstrates that integrating environmental aging and mechanical performance analyses is the most effective strategy for understanding and mitigating environmentally driven failures in polymer composite connectors advancing the broader goal of creating safer, smarter, and more sustainable railway networks.

REFERENCES

1. Wu, S., Ma, X., Zhang, X., Chen, J., Yao, Y., & Li, D. (2024). Investigation into hydrogen induced fracture of cable bolts under deep stress corrosion coupling conditions. Tunnelling and Underground Space Technology, 147, 105729.
2. Yang, H., Shi, Z., Wang, X., Zhang, J., Zhang, R., & Wang, H. (2025). Simulation and Analysis of Electric Thermal Coupling for Corrosion Damage of Metro Traction Motor Bearings. Machines, 13(8), 680.
3. Xie, F. (2007). A study of vibration-induced fretting corrosion for electrical connectors (Doctoral dissertation).
4. Li, J., He, W., Yang, M., Deng, J., & Li, W. (2025). Bidirectional Shear Performance of Corroded Stud Connectors in Steel–Concrete Composite Monorail Track Beams. Buildings, 15(18), 3331.
5. Elayaperumal, K., & Raja, V. S. (2015). Corrosion failures: theory, case studies, and solutions. John Wiley & Sons.
6. Waqas, H. A., Bahrami, A., Amin, F., Sahil, M., & Saud Khan, M. (2024). Numerical modeling and performance evaluation of carbon fiber-reinforced polymer-strengthened concrete culverts against water-induced corrosion. Infrastructures, 9(5), 82.
7. Liu, X., Pei, Z., Feng, Q., & Zhu, Z. (2024). Preload loss in uncoated weathering steel bolted connections considering corrosion and fatigue. Journal of Constructional Steel Research, 221, 108921.
8. Adasooriya, N. D., Hemmingsen, T., & Pavlou, D. (2020). Environment-assisted corrosion damage of steel bridges: a conceptual framework for structural integrity. Corrosion Reviews, 38(1), 49-65.
9. Wang, C. T., Li, W., Xin, G. F., Wang, Y. Q., Yang, X. F., & Guo, Z. A. (2020). Experimental research examining the stray current corrosion of rock bolts in the DC transit system. Experimental Techniques, 44(2), 137-148.
10. Liu, Z., Guo, T., Yu, X., Niu, S., & Correia, J. (2023). Corrosion fatigue assessment of bridge cables based on equivalent initial flaw size model. Applied Sciences, 13(18), 10212.
11. Prasad, S.B., Madhumathy, P., 2021. Long term evolution for secured smart railway communications using internet of things. In: Machine Learning Algorithms for Industrial Applications. Springer, Cham, pp. 285–300

12. Fraga-Lamas, P., Fern´andez-Caram´es, T.M., Castedo, L., 2017. Towards the Internet of smart trains: a review on industrial IoT-connected railways. Sensors 17 (6), 1457.
13. Adebiyi, O.O., Cruz, M., 2018. Green sustainability development for industry internet of things in railway transportation industry. Int. J. Trend Sci. Res. Develop. 3 (1),203–208
14. Perwej, Y., Haq, K., Parwej, F., Mumdouh, M., Hassan, M., 2019. The internet of things (IoT) and its application domains. Int. J. Comp. Appl. 975 (8887), 182.
15. Solanki, A. and Nayyar, A., 2019. Green internet of things (G-IoT): ICT technologies,principles, applications, projects, and challenges. In Handbook of Research on Big Data and the IoT (pp. 379-405). IGI Global
16. Zantalis, F., Koulouras, G., Karabetsos, S., Kandris, D., 2019. A review of machine learning and IoT in smart transportation. Future Internet 11 (4), 94.
17. Mehmood, M.Y., Oad, A., Abrar, M., Munir, H.M., Hasan, S.F., Muqeet, H. and Golilarz, N.A., 2021. Edge computing for IoT-enabled smart grid. Security and Communication Networks, 2021
18. Zhong, G., Xiong, K., Zhong, Z., Ai, B., 2021. Internet of things for high-speed railways. Intelligent Converged Networks 2 (2), 115–132
19. Gharami, S., Prabadevi, B., Bhimnath, A., 2019. Semantic analysis-internet of things,study of past, present, and future of IoT. Electronic Government, Int. J. 15 (2), 144–165
20. Chen, C.W., 2020. Internet of video things: Next-generation IoT with visual sensors. IEEE Internet Things J. 7 (8), 6676–6685
21. S. Pal A. Dorri R. Jurdak Blockchain for IoT Access Control: Recent Trends and Future Research Directions 2021 arXiv preprint arXiv:2106.04808.
22. Wang, Y., Sarkis, J., 2021. Emerging digitalisation technologies in freight transport and logistics: Current trends and future directions. Transp. Res. Part E 148, 102291.
23. Yi, D.L., Liang, D., 2010. A survey of the internet of things. Proc. of ICEBI 358–366
24. Alam, S., Chowdhury, M.M., Noll, J., 2011. Interoperability of security-enabled internet of things. Wireless Pers. Commun. 61 (3), 567–586.
25. Khutey, R., Rana, G., Dewangan, V., Tiwari, A., Dewamngan, A., 2015. Future of wireless technology 6G & 7G. Int. J. Elec. Electron. Res. 3 (2), 583–585
26. Spencer Jr, B.F., Park, J.W., Mechitov, K.A., Jo, H., Agha, G., 2017. Next generation wireless smart sensors toward sustainable civil infrastructure. Procedia Eng. 171, 5–13.
27. Elmeadawy, S. and Shubair, R.M., 2019, November. 6G wireless communications: Future technologies and research challenges. In 2019 international conference on electrical and computing technologies and applications (ICECTA) (pp. 1-5). IEEE
28. Malik, U.M., Javed, M.A., Zeadally, S. and ul Islam, S., 2021. Energy efficient fog computing for 6G enabled massive IoT: Recent trends and future opportunities. IEEE Internet of Things Journal, pp.1-22.
29. Mahmoud, H.H.H., Amer, A.A., Ismail, T., 2021. 6G: A comprehensive survey on technologies, applications, challenges, and research problems. Trans. Emerg. Telecommun. Technol. 32 (4), e4233.
30. Zarembski, A.M., 2014, October. Some examples of big data in railroad engineering. In 2014 IEEE International Conference on Big Data (Big Data) (pp. 96-102). IEEE.
31. Liu, X., Zhang, X., Xue, F., Liao, W., 2010. United Transportation of Railways and Highways Omni distance Tracking System Model under the Internet of Things. In: ICLEM 2010: Logistics For Sustained Economic Development: Infrastructure, pp. 2207–2213.
32. Zhang, R.X., Liu, Z.Y., Guo, J.W., 2011. Research on application of internet of things technology in railway transportation. J. Railway Eng. Soc. 10, 021
33. Xie, Z. and Qin, Y., 2019. High-speed railway perimeter intrusion detection approach based on Internet of Things. Adv. Mech. Eng., 11(2), p.1687814018821511
34. Ai, B., Molisch, A.F., Rupp, M., Zhong, Z.D., 2020. 5G key technologies for smart railways. Proc. IEEE 108 (6), 856–893.
35. Flammini, F., Lin, Z., Vittorini, V., 2020. Roadmaps for AI integration in the rail sector—Rails. ERCIM News 2020 (121).

36. Dirnfeld, R., Flammini, F., Marrone, S., Nardone, R. and Vittorini, V., 2020. Low-power wide-area networks in intelligent transportation: Review and opportunities for smart-railways. In 2020 IEEE 23rd International Conference on Intelligent Transportation Systems (ITSC) (pp. 1-7). IEEE.
37. Wang, L., Von Laszewski, G., Younge, A., He, X., Kunze, M., Tao, J., Fu, C., 2010. Cloud computing: a perspective study. New Generation Computing 28 (2), 137–146.
38. Jadeja, Y. and Modi, K., 2012, March. Cloud computing-concepts, architecture, and challenges. In 2012 International Conference on Computing, Electronics and Electrical Technologies (ICCEET) (pp. 877-880). IEEE
39. Dillon, T., Wu, C. and Chang, E., 2010, April. Cloud computing: issues and challenges.In 2010 24th IEEE international conference on advanced information networking andapplications (pp. 27-33). IEEE
40. Jauro, F., Chiroma, H., Gital, A.Y., Almutairi, M., Shafi'i, M.A. and Abawajy, J.H., 2020.Deep learning architectures in emerging cloud computing architectures: Recent development, challenges and next research trend. Applied Soft Computing, 96, p.106582.
41. Russom, P., 2011. Big data analytics. TDWI best practices report, fourth quarter, 19(4),pp.1-34.
42. Ahmed, E., Yaqoob, I., Hashem, I.A.T., Khan, I., Ahmed, A.I.A., Imran, M., Vasilakos, A.V., 2017. The role of big data analytics in Internet of Things. Comput. Netw. 129,459–471.
43. Bessis, N., Dobre, C. (Eds.), 2014. Big Data and Internet of Things: A Roadmap for Smart Environments (Vol. 546). Springer International Publishing, Basel, Switzerland
44. Li, W., Chen, Z.H. and Sui, L.Y., 2014. Design and Application of Mass Passenger Flow Precautionary and Forecasting System in Rail Transit Based on the Internet of Things Technology. In Applied Mechanics and Materials (Vol. 556, pp. 6366-6369). Trans Tech Publications Ltd.
45. Zhang, W., 2012. Study on internet of things application for high-speed train maintenance, repair, and operation (MRO). In Proceedings of the National Conference on Information Technology and Computer Science (CITCS 2012), Lanzhou, China (pp.16-18).
46. Chapman, L., Warren, E. and Chapman, V., 2016. Using the internet of things to monitor low adhesion on railways. In Proceedings of the Institution of Civil Engineers-Transport (Vol. 169, No. 5, pp. 321-329). Thomas Telford Ltd
47. Karaduman, G., Karakose, M. and Akin, E., 2018. Condition monitoring platform in railways based on IoT. In 2018 International Conference on Artificial Intelligence and Data Processing (IDAP) (pp. 1-4). IEEE
48. Shankar, T., Yamuna, G., Elanchezhian, E.B., 2019. Advanced landslide surveillance system for railway transport accident avoidance using Internet of Things (IoT).J. Comput. Theor. Nanosci. 16 (4), 1701–1705.
49. Mohamed, A., Peng, Q., Abid, M.M., 2020. Integrated maintenance logistics monitoring system for high-speed rail, based on internet of things technology. Eur. TransportTrasporti Europei 2020 (75–6), 1–10.
50. Ling, Z.H.A.O., 2013. Design of railway freight transport security system based on internet of things. J. Chongqing Univ. Technol. (Natural Science) 6, 025.
51. Imdad, M., Jacob, D.W., Mahdin, H., Baharum, Z., Shaharudin, S.M., Azmi, M.S., 2020 .Internet of things (IoT); security requirements, attacks, and counter measures. Indonesian J. Elec. Eng. Computer Sci. 18 (3), 1520–1530
52. Dulebenets, M.A., 2018. A comprehensive multi-objective optimization model for the vessel scheduling problem in liner shipping. Int. J. Prod. Econ. 196, 293–318.
53. Dulebenets, M.A., 2019. A Delayed Start Parallel Evolutionary Algorithm for just-in-time truck scheduling at a cross-docking facility. Int. J. Prod. Econ. 212, 236–258.
54. Safaeian, M., Fathollahi-Fard, A.M., Tian, G., Li, Z., Ke, H., 2019. A multi-objective supplier selection and order allocation through incremental discount in a fuzzy environment. J. Intell. Fuzzy Syst. 37 (1), 1435–1455
55. Fathollahi-Fard, A.M., Dulebenets, M.A., Hajiaghaei-Keshteli, M., Tavakkoli-Moghaddam, R., Safaeian, M., Mirzahosseinian, H., 2021a. Two hybrid metaheuristic algorithms for a dual-channel closed-loop supply chain network design problem in the tire industry under uncertainty. Adv. Eng. Inf. 50, 101418

